Ferro- and Antiferromagnetic Exchange in Decamethylbimetallocenes

Harald Hilbig,[1a] Peter Hudeczek,[1a] Frank H. Köhler,*[,1a] Xiulan Xie,[1c] Pierre Bergerat,[1b] and Olivier Kahn*[,1b]

Anorganisch-chemisches Institut, Technische Universität München, D-85747 Garching, Germany, and Laboratoratoire des Sciences Moléculaires, Institut de Chimie de la Matière Condensée de Bordeaux, UPR CNRS 9048, Avenue du Dr. A. Schweitzer, F-33608 Pessac Cédex, France

Received March 24, 1998

With the aim of studying next-neighbor magnetic interactions in polymeric metallocenes the paramagnetic decamethylbimetallocenes (M′M′) have been chosen as most simple model compounds. They have been synthesized for vanadium, cobalt, and nickel (to yield V′V′, Co′Co′, and Ni′Ni′, respectively) by starting from dilithium and dithallium salts of the fulvalene dianion. The latter have been characterized by ^{13}C NMR spectroscopy. Decamethylbiferrocene has been synthesized as a diamagnetic standard compound, and decamethylbicobaltocenium hexafluorophosphate, as a precursor to Co′Co′. While the methylated M′M′ species were stable when protected from air, the synthesis of the parent binickelocene (Ni′Ni′) was accompanied by the formation of the ternickelocene NiNiNi. According to ^1H NMR spectroscopy NiNi and NiNiNi were antiferromagnetic and underwent ligand exchange to nickelocene and bisfulvalenedinickel. Unlike the usually green nickelocenes Ni′Ni′ was deep red-violet owing to a new band at 528 nm. Measurements of the magnetic susceptibility (χ_m) and the magnetization established a rare example of ferromagnetic interaction within a purely organometallic compound for Co′Co′. By contrast, V′V′ and Ni′Ni′ were antiferromagnetic ($J = -1.6$ and -180 cm^{-1}, respectively, with $\mathbf{H} = -J\mathbf{S}_A\cdot\mathbf{S}_B$). The ^1H and ^{13}C NMR spectra confirmed the expected structures of Co′Co′ and Ni′Ni′, while the synthesis of V′V′-d_8 and ^2H NMR spectroscopy were necessary to fully establish the vanadium compound. Temperature-dependent measurements of the ^1H NMR signal shifts and of χ_m yielded similar J values for Ni′Ni′. MO calculations were carried out for M′M′, and the results were converted into theoretical NMR spectra of the bridging fulvalene ligand depending on the spin-carrying MO. This allowed the full assignment of the NMR signals and showed that the spin is delocalized to more than one MO. The MOs were shown to have different magnetic coupling capabilities, and the different magnetic behavior of M′M′ was attributed to the near-degeneracy of the magnetic orbitals.

Introduction

With novel permanent magnets in view, much effort has been invested during the past decade in the synthesis of molecule-based magnetic materials. In these materials open-shell molecules or centers must be arranged in such a way that the interactions between them end up in spontaneous magnetization. The topic enjoys broad interest, because organic radicals, open-shell transition-metal ions, and combinations of both can be used as building blocks of an ordered solid.[2] Presently, $V(TCNE)_2\cdot{}_2CH_2Cl_2$[3] and $V[Cr(CN)_6]_{0.86}\cdot 2.8H_2O$[4] are the most promising materials which both have a magnetic phase-transition temperature above room temperature. Pure organic polyradicals are less advanced; they will compete after solving the problem of the notorious thermal instability and/or low magnetic phase-transition temperature. As for organometallic compounds, a landmark was established by the discovery of high coercive-field, low-temperature magnets which consist of stacks with alternating radical anions such as tetracyanoethenide and decametallocenium ions.[5]

While these stacks may be regarded as a mixed organic/organometallic approach, surprisingly little is known about combining exclusively organometallic building blocks. Here we wish to reduce this gap by reporting on paramagnetic metallocenes (Cp_2M) which are coupled via the Cp ligands. The metallocenes were chosen because their spin state strongly varies with the metal while the sandwich structure is maintained. The target materials would ideally be polymers consisting of intact sandwiches that experience magnetic interactions. However, often polymers are not well defined. Therefore and since *next*-neighbor interactions are expected to strongly determine the magnetism, we hoped to obtain insight by investigating polymer fragments. The most simple fragments that are derived from

(1) (a) Technische Universität München. (b) Institut de Chimie de la Matière Condensée. (c) On leave from the Fujian Institute of Research of the Structure of Matter, Chinese Academy of Science, Fuzhou, China.

(2) Recent reviews: (a) Miller, J. S.; Epstein A. J. *Chem. Eng. News* **1995**, *Oct. 2*, 30−41. (b) Veciana, J.; Cirujeda, J.; Rovira, C.; Vidal-Gancedo, J. *Adv. Mater.* **1995**, *7*, 221−225. (c) Gatteschi, D. *Adv. Mater.* **1994**, *6*, 635−645. (d) Clement, R.; Lacroix, P. G.; O'Hare, D.; Evans, J. *Adv. Mater.* **1994**, *6*, 794−797. (e) Miller, J. S.; Epstein, A. J. *Angew. Chem., Int. Ed. Engl.* **1994**, *33*, 385−415. (f) Day, P. *Chem. Soc. Rev.* **1993**, 51−57. (g) Kahn, O. *Molecular Magnetism*; VCH Publishers: Weinheim, 1993. (h) Caneschi, A.; Gatteschi, D.; Rey, P. *Progr. Inorg. Chem.* **1991**, *39*, 331−429. (i) Iwamura, H. *Adv. Phys. Org. Chem.* **1990,** *26*, 179−253.

(3) Manriques, J. M.; Yee, G. T.; McLean, R. S.; Epstein, A. J.; Miller J. S. *Science* **1991,** *252*, 1415−1417.

(4) Ferlay, S.; Mallah, T.; Quahès, R.; Veillet, P.; Verdaguer, M. *Nature* **1995**, *378*, 701−703.

(5) (a) Broderick, W. E.; Eichhorn, D. M.; Liu, X.; Toscano, P. J.; Owens, S. M.; Hoffman, B. M. *J. Am. Chem. Soc.* **1995**, *117*, 3641−3642. (b) Miller, J. S.; Vasquez, C.; McLean, R. S.; Reiff, W. M.; Aumüller, A.; Hünig, S. *Adv. Mater.* **1993**, *5*, 448−450. (c) See also earlier work cited by both groups.

S0020-1669(98)00332-2 CCC: $15.00
Published on Web 07/30/1998

Chart 1

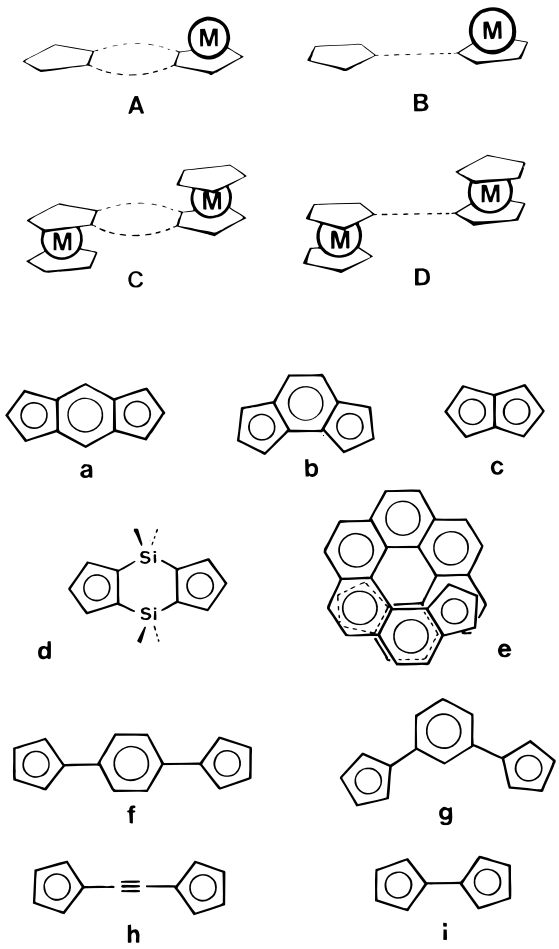

the polymer repeat units of type **A** and **B** in Chart 1 are the dinuclear metallocenes **C** and **D**. In addition, Chart 1 lists bridged Cps which have been used for the synthesis of **C** and **D** as far as neutral species with two paramagnetic centers are concerned.[6] Detailed magnetic studies were reported mainly by Miller and associates[6a,i] and ourselves.[6b,g]

Starting from the doubly silyl-bridged ligand **d** we have investigated extended series of homo- and heterometallic derivatives. They revealed that the interaction mechanisms, which successfully explained the magnetic interaction of bridged coordination compounds,[7] are not applicable to bridged metallocenes. Rather, the similarity to organic diradicals was pointed out. Metallocenes may be regarded as thermally stable reduced-spin analogues of organic radicals, regardless whether they are coupled or mononuclear, because the corresponding spin-carrying MOs are similar.[8] Another remarkable conclusion was that the antiferromagnetic interaction between the silyl-bridged metallocenes was governed by hyperconjugation such that the bridges serve as a spin valve which is closed when the ligand **d** is flat.

A stronger magnetic interaction between neighboring metallocenes could be expected when the fulvalene-type ligand **i** was used. In the resulting bimetallocenes there is just one bond between the paramagnetic building blocks, and it should be possible to vary the interaction by adjusting the spin density on C1/10 of **i**. This prompted us to synthesize paramagnetic bimetallocenes, to study their magnetic properties, and to analyze the distribution of the unpaired spin within the molecules. Whereas all open-shell sandwiches derived so far from the ligands in Chart 1 display antiferromagnetic (if any) interaction, a ferromagnet was now obtained as established in the following report.

Scheme 1[a]

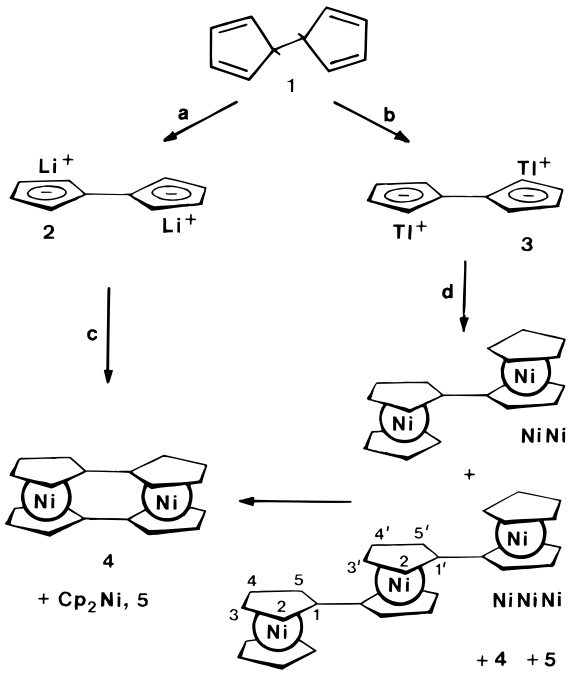

[a] Key: (a) *n*-BuLi; (b) $[Tl(OMe)]_4$; (c) $NiBr_2(THF)_n$; (d) Cp-Ni[P(OMe)$_3$].

Results

Syntheses. The most simple and general approach to bimetallocenes that does not conflict with the high reactivity expected for open-shell metallocenes starts from the fulvalene dianion. As shown in Scheme 1, it can be obtained as the dilithium salt **2**[9] or the dithallium salt **3**.[10] Since **3** is insoluble it is difficult to characterize. In particular, this applies for a conceivable contamination with CpTl which is hard to detect, e.g., by elemental analysis. The ^{13}C CP MAS NMR spectrum[11] of **3** approximately showed a 1/2/2 pattern (Table 1) of which

(6) Recent contributions except for the plethora of ferrocenium derivatives are: (a) Manriquez, J. M.; Ward, M. D.; Reiff, W. M.; Calabrese, J. C.; Jones, N. L.; Carroll, P. J.; Bunel, E. E.; Miller, J. S. *J. Am. Chem. Soc.* **1995**, *117*, 6182−6193. (b) Atzkern, H.; Bergerat, P.; Fritz, M.; Hiermeier, J.; Hudeczek, P.; Kahn, O.; Kanellakopulos, B.; Köhler, F. H.; Ruhs, M. *Chem. Ber.* **1994**, *127*, 277−286. (c) Gilbert, A. M.; Katz, T. J.; Geiger, W. E.; Robben, M. P.; Rheingold, A. L. *J. Am. Chem. Soc.* **1993**, *115*, 3199−3211. (d) Stephan, M.; Davis, J. H., Jr.; Meng, X.; Chase, K. J.; Hauss, J.; Zenneck, U.; Pritzkow, H.; Siebert, W.; Grimes, R. N. *J. Am. Chem. Soc.* **1992**, *114*, 5214−5221. (e) Schottenberger, H.; Ingram, G.; Obendorf, D. *J. Organomet. Chem.* **1992**, *426*, 109−119. (f) Schottenberger, H.; Ingram, G.; Obendorf, R.; Tessadri, R. *Synlett* **1991**, 905−907. (g) Atzkern, H.; Hiermeier, H.; Kanellakopulos, B.; Köhler, F. H.; Müller, G.; Steigelmann, O. *J. Chem Soc., Chem. Commun.* **1991**, 997−999. (h) Desbois, M.-H.; Astruc, D.; Guillin, J.; Varret, F.; Trautwein, A. X.; Villeneuve, G. *J. Am. Chem. Soc.* **1989**, *111*, 5800−5809. (i) Manriquez, J. M.; Ward, M. D.; Calbrese, J. C.; Fagan, P. J.; Epstein, A. J.; Miller, J. S. *Mol. Cryst. Liq. Cryst.* **1989**, *176*, 527−534. (j) McManis, G. E.; Nielson, R. M.; Weaver, M. J. *Inorg. Chem.* **1988**, *27*, 1827−1829. (k) Bunel, E. E.; Valle, L.; Jones, N. L.; Carroll, P. J.; Gonzales, M.; Munos, N.; Manriquez, J. M. *Organometallics* **1988**, *7*, 789−791.

(7) Kahn, O. *Molecular Magnetism*; VCH Publishers: Weinheim, 1993; Chapters 7 and 8.

(8) (a) Atzkern, H.; Bergerat, P.; Beruda, H.; Fritz, M.; Hiermeier, J.; Hudeczek, P.; Kahn, O.; Köhler, F. H.; Paul, M.; Weber, B. *J. Am. Chem. Soc.* **1995**, *117*, 997−1011. (b) Köhler, F. H.; Geike, W. A. *J. Organomet. Chem.* **1987**, *328*, 35−47.

Table 1. NMR Results of Diamagnetic Fulvalenediyl Derivatives

position[a] of nuclei	**2**[b]	**3**[c]	Fe′Fe′ [d]	[Co′Co′]$^{2+}$ [e]
H2/5			3.73	5.55
H3/4			3.66	5.48
CH_3	121.7	125.6	1.72	1.79
C1	99.3 (156.1)	107.3	83.2	93.5
C2/5	101.3 (155.5)	111.5	71.7	84.1
C3/4			68.4	89.8
CCH_3			80.2	99.7
CH_3			11.0	10.4

[a] For numbering see Scheme 1. [b] In DMSO-d_6. ^1J(CH) values in Hz in parentheses. [c] CP MAS NMR. [d] In C_6D_6. [e] In acetonitrile-d_3.

the signal at 111.5 ppm was 5−10% bigger than that of C2/5. We conclude that the routine preparation of **3** also gives some CpTl with $\delta(^{13}C) \sim 111$, a value which is not far from that found in solution.[12] Since $\delta(^{13}C1) = 125.6$ did not agree with the most-shifted signal of the dilithio derivative **2** given in the literature[9d] (103.2 ppm), we have remeasured the ^{13}C NMR spectrum of **2**. As can be seen in Table 1, the signal of C1 appears in the expected range. In addition we found a signal at 103.0 ppm which stems from Cp^-.[12] This demonstrates that usually **2** and **3** contain Cp^- and that one of the signal shifts published previously[9d] did not belong to **2**.

In an attempt to synthesize binickelocene (NiNi) a mixture of **2** and Cp^- was reacted with solvated nickel(II) bromide. Although this approach proved successful in similar cases,[6b,g,13] bisfulvalenedinickel[14] (**4**) and nickelocene (**5**) were obtained rather than NiNi (Scheme 1). The result was improved when **3** and CpNiCl[P(OCH$_3$)$_3$][15] were combined.[16] After rapid workup the deep red-violet hexane-soluble fraction gave the ^1H NMR spectrum in Figure 1a. It shows the presence of four paramagnetic sandwich compounds: Cp_2Ni, bisfulvalenedinickel, NiNi, and most probably ternickelocenene (NiNiNi). The signals of the first two compounds were identified by comparison with authentic samples. The number and the relative areas of the remaining signals are in accord with what we expect for NiNi and NiNiNi. In particular, the resonances appear in ranges that are characteristic of antiferromagnetically coupled nickelocenes (for details see below). The formation of NiNi was confirmed by mass spectroscopy, which showed the molecular ions with a signal pattern that was virtually identical with the calculated intensities.

The freshly prepared sample which contained NiNi, Cp_2Ni, NiNiNi, and bisfulvalenedinickel in the ratio 43/6/3/1 (signal areas in Figure 1, upper trace) slowly changed its color from violet to brown, and a dark precipitate appeared. ^1H NMR spectroscopy showed that the mixed-ligand compounds NiNi and NiNiNi disappeared in favor of Cp_2Ni and bisfulvalenedinickel (Figure 1, lower trace); the formation of polynickelocenylene was not excluded. We ascribe this to ligand exchange[17] which did not allow us to purify NiNi by crystallization and chromatography.

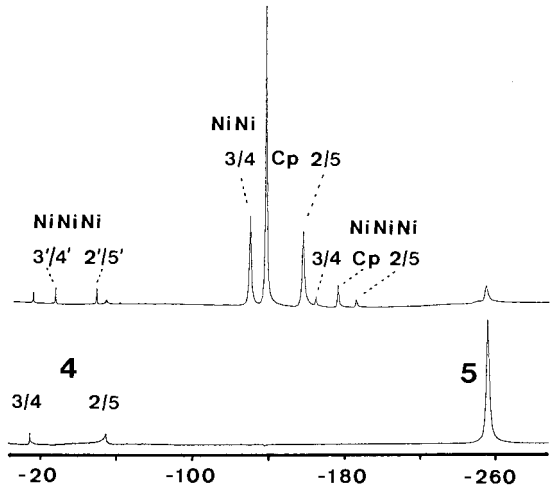

Figure 1. ^1H NMR spectra of the nickel sandwiches shown in Scheme 1. Upper trace: After reaction **d** of Scheme 1. Lower trace: The same solution 8 weeks later. Solvent C_6D_6, temperature 293 K, scale in ppm. For acronyms and numbering see Scheme 1.

Scheme 2[a]

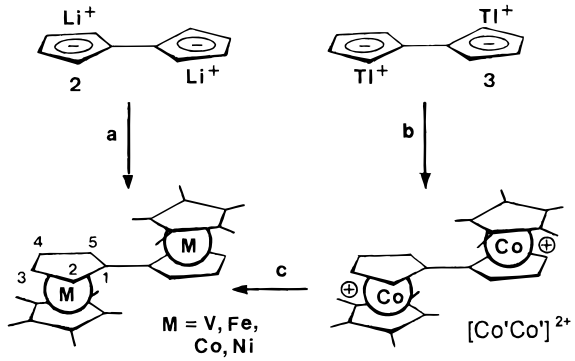

[a] Key: (a) $(C_5Me_5)Li$, $VCl_3(THF)_3$, Zn or $(\eta^5\text{-}C_5Me_5)Co(acac)$ or $(\eta^5\text{-}C_5Me_5)Ni(acac)$; (b) $[(\eta^5\text{-}C_5Me_5)CoCl]_2$; (c) Na/Hg.

When pentamethylcyclopentadienyl (η^5-C_5Me_5) was used as a terminal ligand the corresponding decamethylbinickelocene (Ni′Ni′, as distinct from NiNi = binickelocene; the prime is also used for other decamethylbimetallocenes) could be isolated. As summarized in Scheme 2, Ni′Ni′ and Co′Co′ were obtained from the reaction of **2** with $(\eta^5\text{-}C_5Me_5)M(acac)$ (M = Co, Ni; acac = acetylacetonate),[18] while V′V′ and the diamagnetic reference compound Fe′Fe′ were synthesized from the metal(II) halides and a mixture of **2** and $(C_5Me_5)Li$. The synthesis of Cr′Cr′ was also attempted on different routes. The crude product obtained from the reaction of **2** with $[(\eta^5\text{-}C_5Me_5)CrCl]_2$ showed ^1H NMR signals of appropriate relative intensities in the ranges expected for chromocenes[8] at 330 and 350 ppm for the fulvalene protons and at −6 ppm for the $(\eta^5\text{-}C_5Me_5)$ protons. However, we were unable to isolate Cr′Cr′, presumably again due to ligand exchange as in the case of NiNi. To obtain reliable magnetic data, V′V′, Co′Co′, and Ni′Ni′ were purified by

(9) (a) LeVanda, C.; Bechgaard, K.; Cowan, D. O.; Mueller-Westerhoff, U. T.; Eilbracht, P.; Candela, G. A.; Collins, R. L. *J. Am. Chem. Soc.* **1976**, *98*, 3181−3187. (b) Smart, J. C.; Curtis, C. J. *Inorg. Chem.* **1977**, *16*, 1788−1790. (c) Vollhardt, K. P. C.; Weidmann, T. W.; *Organometallics* **1984**, *3*, 82−86. (d) Escher, A.; Rutsch, W.; Neuenschwander, M. *Helv. Chim. Acta* **1986**, *69*, 1644−1654. (e) Curtis, C. J.; Haltiwanger, R. C. *Organometallics* **1991**, *10*, 3220−3226.
(10) (a) Spink, W. C.; Rausch, M. D. *J. Organomet. Chem.* **1986**, *308*, C1−C4. (b) Rausch, M. D.; Spink, W. C.; Conway, B. G.; Rogers, R. D.; Atwood, J. L. *J. Organomet. Chem.* **1990**, *383*, 227−252.
(11) Blümel, J.; Hudeczek, P. Unpublished results.
(12) Fischer, P.; Stadelhofer, P.; Weidlein, J. *J. Organomet. Chem.* **1976**, *116*, 65−73.
(13) (a) Atzkern, H.; Huber, B.; Köhler, F. H.; Müller, G.; Müller, R. *Organometallics* **1991**, *10*, 238−244. (b) Atzkern, H.; Hiermeier, J.; Köhler, F. H.; Steck, A. *J. Organomet. Chem.* **1991**, *408*, 281−296.
(14) Smart, J. C.; Pinsky, B. L. *J. Am. Chem. Soc.* **1977**, *99*, 956−957.
(15) Harder, V.; Werner, H. *Helv. Chim. Acta* **1973**, *56*, 1620−1629.
(16) Hudeczek, P. Diploma Thesis, Technische Universität München, 1990.
(17) Switzer, M. E.; Rettig, M. F. *J. Chem. Soc., Chem. Commun.* **1972**, 687−688; *Inorg. Chem.* **1974**, *13*, 1975−1981.
(18) Bunel, E. E.; Valle, L.; Manriquez, J. M. *Organometallics* **1985**, *4*, 1680−1682.

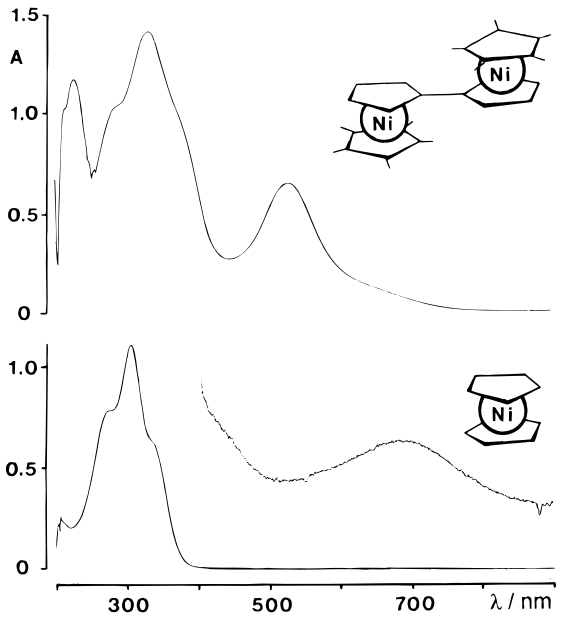

Figure 2. Electronic spectra of Ni′Ni′ and nickelocene dissolved in *n*-hexane (1.0443 and 1.0086 mol L^{-1}, respectively) at 25 °C.

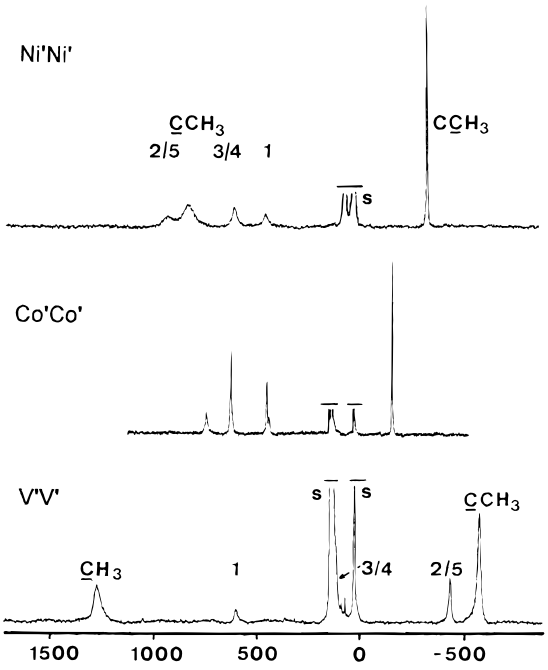

Figure 3. ^{13}C NMR spectra of Ni′Ni′ in THF at 337 K and Co′Co′ and V′V′ in toluene-d_8 at 306 K; *s* = solvent, scale in ppm. For acronyms and numbering see Scheme 2. The signal assignment for Co′Co′ is analogous to that for Ni′Ni′.

repeated crystallization, until the ^1H NMR spectra showed no other paramagnetic species and satisfactory elemental analyses were obtained. When Fe′Fe′ was isolated by using medium-pressure liquid chromatography, a separate band turned out to contain decamethylterferrocene (Fe′FeFe′) as evidenced by NMR spectroscopy. In all cases the purification procedure lowered the yield to 15−25%.

Alternatively Co′Co′ was synthesized starting from the dithallium derivative **3** and $[(\eta^5\text{-}C_5Me_5)CoCl]_2$[19] (Scheme 2). This reaction did not yield a hexane-soluble organometallic compound. Instead aqueous workup gave diamagnetic $[Co'Co']^{2+}$ which was isolated as PF_6^- salt in 95% yield. The appearance of metallic thallium indicated that Co′Co′ had been oxidized by Tl^+. The reduction of $[Co'Co']^{2+}$ with an excess of sodium amalgam afforded the desired Co′Co′ in 88% yield. Parallel to our preliminary work[20] Astruc et al.[21] synthesized $[Co'Co']^{2+}$ and Fe′Fe′.[21a] These authors also reported leading details on $[Fe'Fe']^+$,[21b] $[Fe'Fe']^{2+}$,[21c] and $[Rh'Rh']^{2+}$.[21a]

The paramagnetic compounds are very air-sensitive and deeply colored, while orange Fe′Fe′ is only slightly air-sensitive and yellow $[Co'Co']^{2+}$ is air-stable. The neutral decamethylbimetallocenes were readily soluble in hydrocarbons and ethers; their mass spectra were in accord with the anticipated structure.

As for the color of the new compounds the most striking difference between the bimetallocenes and the mononuclear metallocenes was observed for nickel: while the binickelocenes NiNi and Ni′Ni′ are deep red-violet, nickelocene and alkylated derivatives are green, and phenylated nickelocenes are yellow to brown.[22] The electronic spectra of Ni′Ni′ and Cp_2Ni are shown in Figure 2. Cp_2Ni has strong absorptions between 230 and 370 nm and very weak bands near 420 and 690 nm in accord with previous reports.[23] For Ni′Ni′ the strong bands are broader and shifted 20−50 nm to lower energy due to methyl substitution.[23d,24] New strong bands appear at 216 and 528 nm (accompanied by a shoulder above 600 nm), the latter being responsible for the deep red-violet color. We ascribe these features to the simultaneous excitations of both Ni′ fragments and magnetic exchange that greatly enhances the intensity of an electron excitation which is spin-forbidden in mononuclear nickelocenes.[25]

The NMR spectra of Fe′Fe′ and $[Co'Co']^{2+}$ gave the expected number of signals (Table 1). When the fulvalene protons were assigned as published for biferrocene[26] (δ(H2/5) > δ(H3/4)), the C,H-COSY spectrum led to δ(C2/5) > δ(3/4), in accord with other undistorted neutral fulvalene complexes.[27] Surprisingly, the C,H-COSY spectrum of $[Co'Co']^{2+}$ revealed that, unlike for Fe′Fe′, the stronger shifted signal of H2−5 was correlated with the less-shifted signal of C2−5. A selective heteronuclear NOE difference experiment[27] proved that the signal of C2/5 was less shifted than that of C3/4.

Paramagnetic NMR Spectra. While the ^1H NMR spectra of V′V′, Co′Co′, and Ni′Ni′ could be recorded straightforwardly, a large sample concentration and a solenoid probe head were used to observe the ^{13}C NMR spectra in Figure 3. In almost all cases strong shifts overcompensated the large widths of the signals so that the spectral resolution allowed us to deduce useful information. Since this information refers to the effect of the unpaired electrons on the experimental signal shifts, they were

(19) Kölle, U.; Khouzami, F.; Fuss, B. *Angew. Chem., Int. Ed. Engl.* **1982**, *21*, 131.
(20) Hudeczek, P.; Köhler, F. H. *Organometallics* **1992**, *11*, 1773−1775.
(21) (a) Rittinger, S.; Buchholz, D.; Delville-Desbois, M.-H.; Linarès, J.; Varret, F.; Boese, R.; Zsolnai, L. M.; Huttner, G.; Astruc, D. *Organometallics* **1992**, *11*, 1454−1456. (b) Delville, M.-H.; Rittinger, S.; Astruc, D. *J. Chem. Soc., Chem. Commun.* **1992**, 519−520. (c) Delville, M.-H.; Robert, F.; Gouzerh, P.; Linarès, J.; Boukheddaden, K.; Varret, F.; Astruc, D. *J. Organomet. Chem.* **1993**, *451*, C10−C12.
(22) Köhler, F. H.; Matsubayashi, G. *Chem. Ber.* **1976**, *109*, 329−336.
(23) (a) Scott, D. R.; Becker, R. S. *J. Chem. Phys.* **1961**, *35*, 516−531. (b) Prins, R.; Van Voorst, J. D. W. *J. Chem. Phys.* **1968**, *49*, 4665−4673. (c) Traverso, O.; Rossi, R. *Inorg. Chim. Acta* **1974**, *10*, L7−L8. (d) Gordon, K. R.; Warren, K. D. *Inorg. Chem.* **1978**, *17*, 987−994.
(24) Ketkov, S. Yu; Domrachev, G. A.; Mar'in, V. P. *Metallorg. Khim.* **1991**, *4*, 392−396.
(25) McCarthy, P. J.; Güdel, H. K. *Coord. Chem. Rev.* **1988**, *88*, 69−131.
(26) Izumi, T.; Kasahara, A. *Bull. Chem. Soc. Jpn.* **1975**, *48*, 1955−1956.
(27) Meyerhoff, J. D.; Nunlist, R.; Tilset, M.; Vollhardt, K. P. C. *Magn. Reson. Chem.* **1986**, *24*, 709−712.

Table 2. Paramagnetic ^{1}H, ^{2}H, and ^{13}C NMR Signal Shifts[a] of the Decamethylbimetallocenes M′M′ Dissolved in Toluene-d_8

position[a] of nuclei	V′V′	Co′Co′	Ni′Ni′
H2/5	319.0 (4.60)	−60.5 (0.12)	−122.4 (0.48)
D2/5	322.2 (0.12)[c]		
H3/4	319.0 (4.60)	−39.3 (0.08)	−100.6 (0.38)
D3/4	318.4 (0.12)[c]		
CH_3	111.1 (0.95)	36.7 (0.03)	118.0 (0.30)
C1	511 (1.00)	349 (0.85)	373 (1.4)
C2/5	−509 (0.80)	669 (1.00)	862 (4.5)
C3/4	44 (0.40)	376 (0.43)	543 (1.6)
CCH_3	−658 (1.20)	542 (0.55)	753 (3.5)
CCH_3	1252 (2.30)	−173 (0.12)	−342 (0.4)

[a] In ppm relative to the corresponding shifts of Fe′Fe′ (Table 1). ^{1}H NMR data at 298 K. ^{13}C NMR data at 306 K (V′V′ and Co′Co′) and at 337 K (Ni′Ni′). Signal half-widths in kHz in parentheses. [b] For numbering see Scheme 2. [c] At 306 K; assignment interchangeable.

converted to paramagnetic signal shifts δ^{para} by referencing to the corresponding signal shifts of Fe′Fe′. The δ^{para} values and the signal half-widths are collected in Table 2.

The signal assignment was based on the relative intensities and on the fact that for cobaltocenes and nickelocenes the signals of the five-membered ring-C atoms appear at high frequency while those of the methyl-C atoms and of the five-membered ring proton appear at low frequency.[8b,28] For Co′Co′ this was supported by the quartet due to the one-bond C,H coupling of the CH_3 groups. Vanadocenes[8b,28] should have shift signs that are opposite to those just mentioned for cobaltocenes and nickelocenes. This established the (η^5-C_5Me_5) signals of V′V′ while the remaining signals were assigned to the fulvalene ligand. In the case of V′V′ the fulvalene signals required special attention because they were strongly split in the ^{13}C NMR spectrum whereas only one signal was found for H2−5. This could be due to two reasons: (i) The expected signal splitting was too small to be resolved. (ii) One signal coincided with that of (η^5-C_5Me_5) or the solvent. The coincidence of para- and diamagnetic NMR signals can be removed when the temperature dependence of their shifts is sufficiently different. However, variable-temperature NMR spectra showed no improvement. Therefore the fulvalene ligand of V′V′ was deuteriated to give V′V′-d_8. As can be seen in Figure 4, the fulvalene signal splits when passing from the ^{1}H NMR spectrum of V′V′ (Figure 4A) to the ^{2}H NMR spectrum of V′V′-d_8 (Figure 4C), and no signal appears in the methyl region (110 ppm). Accordingly, the ^{1}H NMR spectrum of V′V′-d_8 (Figure 4B) shows the residual fulvalene protons and those of (η^5-C_5Me_5). In these experiments the ^{2}H NMR signal narrowing was exploited that we worked out previously.[29] The signals of all nuclei in the fulvalene positions 2/5 and 3/4 (Table 2, Figures 3 and 4) were distinguished on the basis of arguments given in the Discussion.

Temperature-dependent ^{1}H NMR measurements of V′V′, Co′Co′, and Ni′Ni′ indicated different behavior. This followed from the reduced paramagnetic signal shifts $\vartheta = \delta^{para} \times T/T_s$ (T and T_s are the measuring and standard temperatures, respectively; here we set $T_s = 298$ K) given in Figure 5. Note that ϑ is proportional to $\chi_m T$ (χ_m is the molar magnetic susceptibility; see also Discussion) and would thus be constant

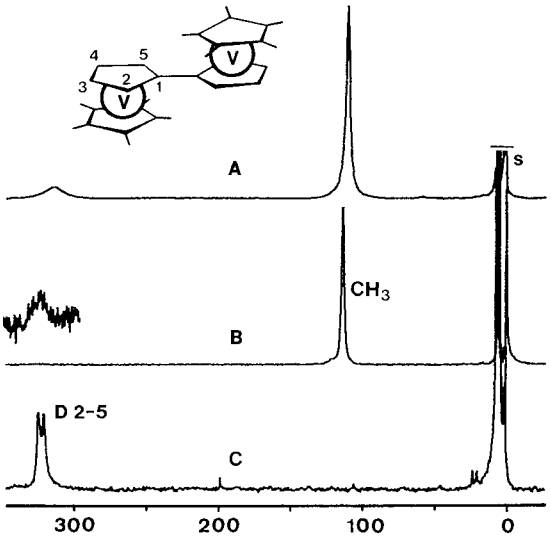

Figure 4. ^{1}H NMR spectra of V′V′ in toluene-d_8 at 306 K (A) and of V′V′-d_8 in C_6D_6 at 298 K (B) and ^{2}H NMR spectrum of V′V′-d_8 in toluene at 298 K (C); s = solvent, scale in ppm.

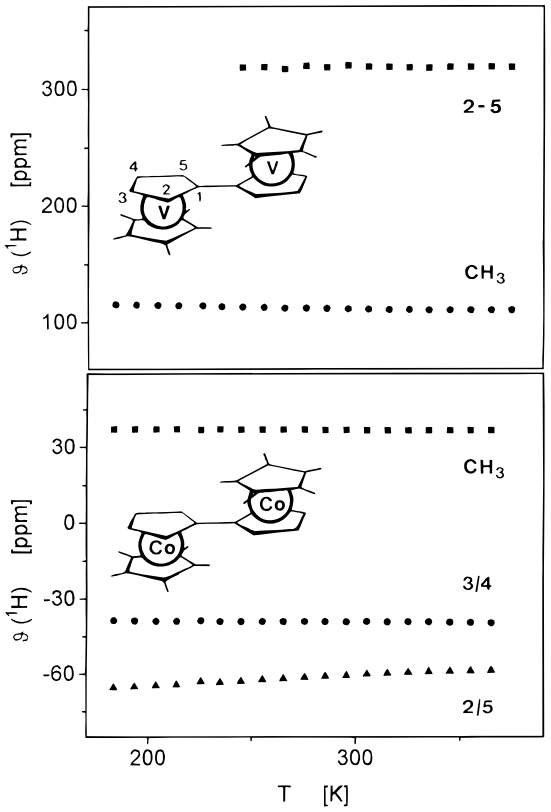

Figure 5. Temperature dependence of the proton signals of Co′Co′ and V′V′ visualized by the reduced paramagnetic signal shifts (see text).

if the Curie law held. This applied to V′V′ (Figure 5) which seemed to behave like vanadocene.[30] However, weak magnetic exchange could not be excluded in this way, owing to the limited temperature range. For Co′Co′ (Figure 5) ϑ was also fairly constant in contrast to substituted mononuclear cobaltocenes which were investigated previously.[31] Finally, all $|\vartheta|$ values

(28) (a) Köhler, F. H.; Doll, K.-H.; Prössdorf, W. *Angew. Chem., Int. Ed. Engl.* **1980**, *19*, 479−480. (b) Köhler, F. H.; Doll, K.-H. *Z. Naturforsch. B: Chem. Sci.* **1982**, *37*, 144−150.
(29) (a) Hebendanz, N.; Köhler, F. H.; Scherbaum, F.; Schlesinger, B. *Magn. Reson. Chem.* **1989**, *27*, 798−802. (b) Blümel, J.; Hofmann, P.; Köhler, F. H. *J. Magn. Reson.* **1993**, *31*, 2−6.
(30) Eicher, H.; Köhler, F. H.; Cao, R. *J. Chem. Phys.* **1987**, *86*, 1829−1835.
(31) Eicher, H.; Köhler, F. H.; *Chem. Phys.* **1988**, *128*, 297−309.

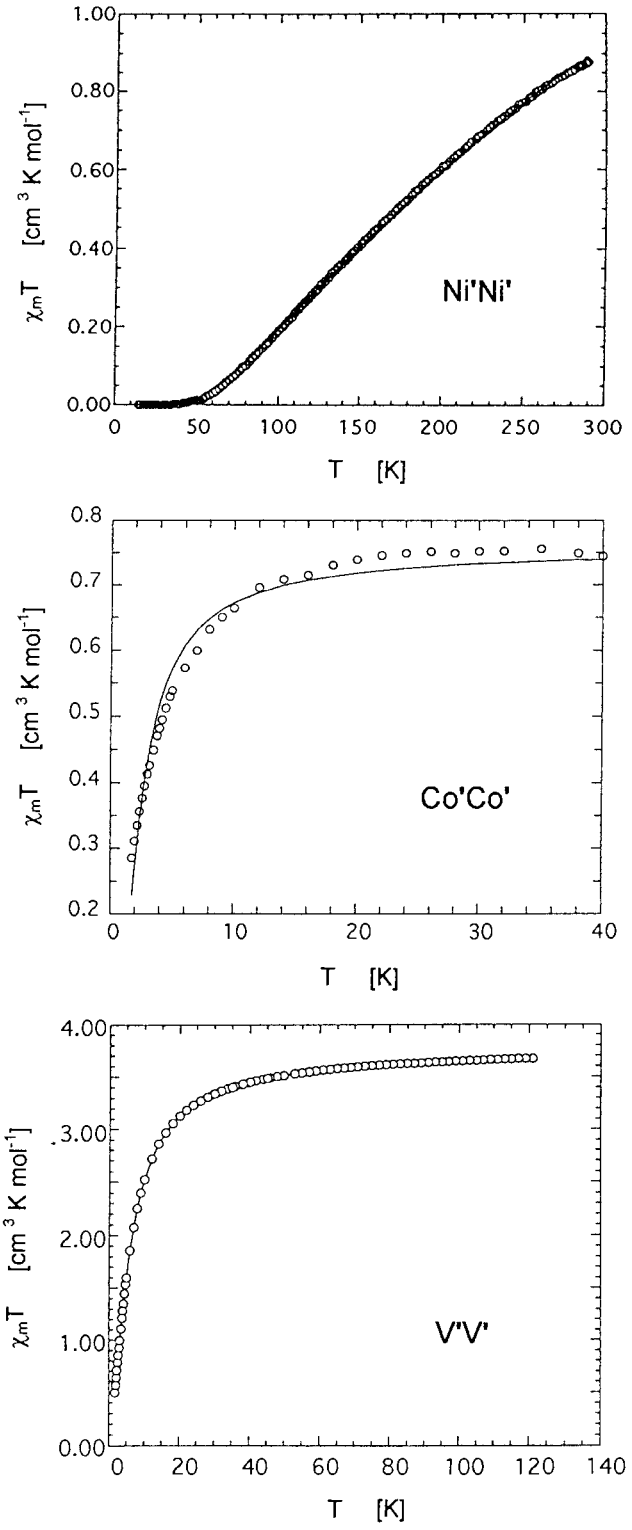

Figure 6. $\chi_m T$ versus T diagrams for V′V′, Ni′Ni′, and Co′Co′. Best fit curves are given with the experimental points; for Ni′Ni′ the curve is completely covered by the points.

of Ni′Ni′ decreased with the temperature which is indicative of antiferromagnetic interaction (see Discussion and Figure 13).

Solid State Magnetic Measurements. The temperature dependencies of the magnetic susceptibility of V′V′, Co′Co′, and Ni′Ni′ are shown in Figure 6 in the form of $\chi_m T$ versus T plots. For V′V′ $\chi_m T$ is equal to 3.68 cm^3 K mol^{-1} at room temperature, which corresponds to what is expected for two isolated $S_V = {}^3/_2$ local spins. As T is lowered, $\chi_m T$ first remains constant down to ca. 150 K, then decreases more and more rapidly, and eventually tends to zero as T approaches the absolute zero. This behavior is characteristic of weak antiferromagnetic interaction. The spin Hamiltonian when applying a magnetic field **H** may be written as

$$\mathbf{H} = -J\mathbf{S}_A\cdot\mathbf{S}_B + D(\mathbf{S}_{A,z}{}^2 + \mathbf{S}_{B,z}{}^2) + g\beta(\mathbf{S}_A + \mathbf{S}_B)\cdot H \quad (1)$$

where the first term in the right-hand side describes the spin interaction, the second term the local anisotropy of the V^{2+} ions (D is the axial zero-field splitting parameter), and the last term the Zeeman perturbation. The other symbols have their usual meaning. A theoretical expression of $\chi_m T$ can be easily deduced from eq 1, and the least-squares fitting of the experimental data leads to $J = -1.58$ cm^{-1}, $D = 2.5$ cm^{-1}, and $g = 1.97$. The agreement factor defined as $R = \Sigma[(\chi_m T)^{cal} - (\chi_m T)^{obs}]^2/\Sigma[(\chi_m T)^{obs}]^2$, which is then equal to 9×10^{-5}.

Let us now consider the Ni′Ni′ case. $\chi_m T$ is equal to 0.94 cm^3 K mol^{-1} at room temperature, which is much less than expected for two isolated $S_{Ni} = 1$ local spins, and it decreases as T is lowered. The compound becomes diamagnetic below ca. 50 K. The χ_m versus T curve shows a rounded maximum at about 240 K, which is characteristic of a strong antiferromagnetic interaction. The least-squares fitting of the experimental data with the theoretical expression of $\chi_m T$ deduced from eq 1 leads to $J = -180$ cm^{-1} and $g = 1.99$. The local anisotropy of the Ni^{2+} ions in the present case is masked by the magnitude of $|J|$.

The case of Co′Co′ is more complicated. $\chi_m T$ is equal to 0.78 cm^3 K mol^{-1} at room temperature and decreases continuously as T is lowered. The $\chi_m T$ value at 1.7 K is 0.28 cm^3 K mol^{-1}. Two hypotheses may be considered to interpret these magnetic susceptibility data: (1) The intramolecular interaction between the $S_{Co} = {}^1/_2$ local spins is weakly antiferromagnetic. Least-squares fitting of the experimental data then leads to a ground singlet-exited triplet energy gap of $J = -3.08$ cm^{-1}. The agreement factor, however, is not satisfying ($R = 2 \times 10^{-3}$). The introduction of an anisotropic interaction term of the form $\mathbf{S}_{Co}\cdot\mathbf{D}_{Co}\cdot\mathbf{S}_{Co}$ (where $\mathbf{D}_{Co}$ is a traceless tensor) might slightly improve the fitting. (2) The intramolecular interaction is strongly ferromagnetic, and the population of the excited singlet state is very weak, even at room temperature ($J > 300$ cm^{-1}). The decrease of $\chi_m T$ as T is lowered would then arise from a zero-field splitting of the ground triplet state. The experimental data can be simulated with such a model. The axial zero-field splitting parameter in the ground triplet state is equal to 12.5 cm^{-1}, and g is 1.72. The agreement factor is then equal to 9×10^{-4}. The introduction of a rhombic zero-field splitting parameter may further improve the model.

The field dependence of the magnetization, $M = f(H)$, at 1.7 K was also investigated in order to obtain more information on the electronic structure of the compounds V′V′ and Co′Co′. The results are presented in the form not only of $M = f(H)$, but also of $\chi_d = f(T)$ curves, where χ_d denotes the differential susceptibility $\partial M/\partial H$.

The two curves for V′V′ are shown in Figure 7. In the absence of local anisotropy, three inflection points in the $M = f(H)$ curve should be observed, corresponding to the crossover between the states $S = 0$ and 1, $S = 1$ and 2, and $S = 2$ and 3, respectively. The local anisotropy, which is of the same order of magnitude as $|J|$, mixes the spin states, and a unique smooth transition is expected. The experimental data are in line with these predictions. The inflection is seen in the $M = f(H)$ curve, as is the maximum in the $\chi_d = f(H)$ curve at about 40 kOe. A

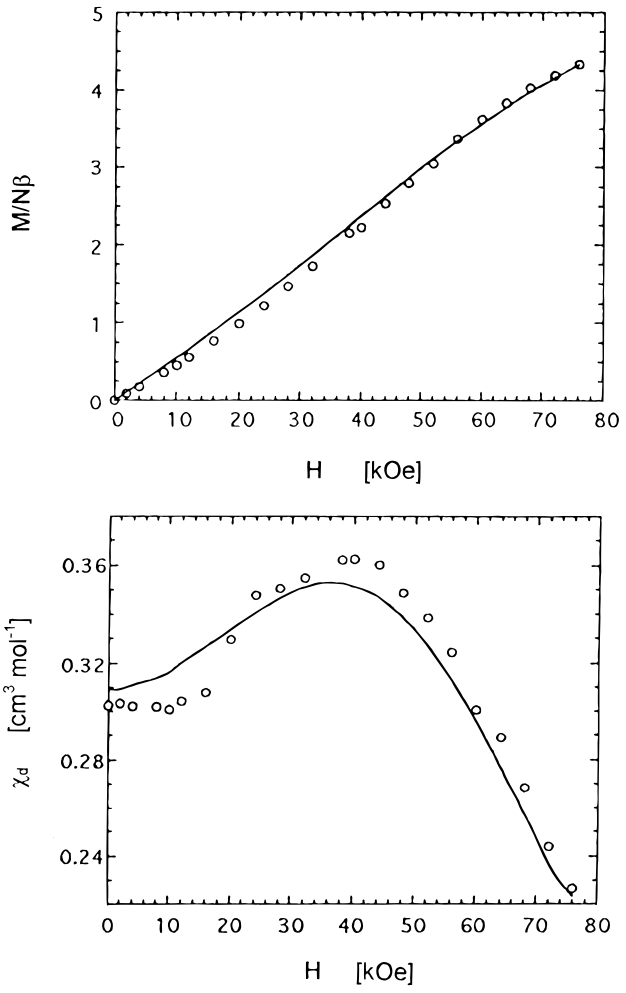

Figure 7. $M = f(H)$ and $\chi_d = f(H)$ curves, with $\chi_d = \partial M/\partial H$, for V′V′. Open circles represent the experimental data. The curves are obtained from least-squares fitting of the data (see text).

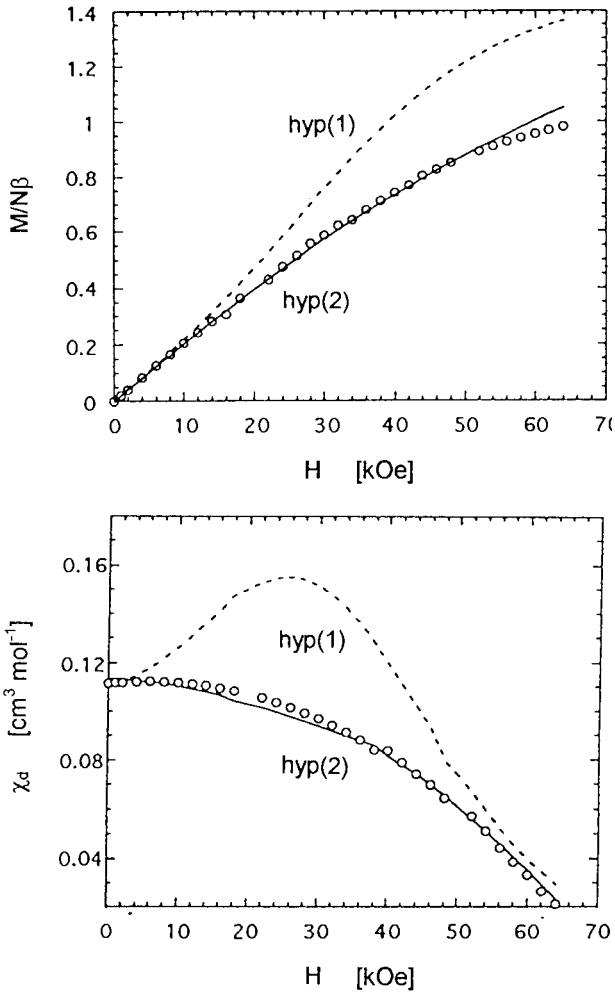

Figure 8. $M = f(H)$ and $\chi_d = f(H)$ curves, with $\chi_d = \partial M/\partial H$, for Co′Co′. Open circles represent the experimental data. The broken curves are those expected for antiferromagnetic interaction (hyp(1)), and the full curves are obtained from least-squares fitting of the data for ferromagnetic interaction (hyp(2)) (see text).

theoretical expression of the magnetization may be derived.[32] The fitting of the magnetization data leads to J, D, and g values which are in very close agreement with the values deduced from the temperature dependence of the magnetic susceptibility.

For the V′V′ compound the magnetization data nicely confirm the susceptibility data. On the other hand, for the Co′Co′ compound the magnetization data allow to decide which of the two hypotheses presented above is valid. As a matter of fact, in hypothesis (1) M should exhibit an inflection point corresponding to the crossover between the singlet state and the $M_s = -1$ Zeeman component of the triplet state, and therefore χ_d should exhibit a maximum. An antisymmetric interaction might mix the spin states and suppress the inflection in the $M = f(H)$ curve. Such an interaction, however, is not compatible with the very likely presence of an inversion center in the molecule. In contrast, in hypothesis (2) M should exhibit no inflection point, and χ_d should decrease continuously as H increases. The experimental data for M and χ_d are shown in Figure 8 along with the theoretical curves expected for hypotheses (1) and (2) (hyp(1) and hyp(2) in Figure 8), respectively. These magnetization curves unambiguously indicate that Co′Co′ has a spin triplet ground state, which is well separated in energy ($J > 300$ cm^{-1}) from the excited singlet state. Probably, only magnetization data could provide this information.

In what precedes, intermolecular (through space) interactions were assumed to be negligibly weak as compared to intramolecular (through bond) interactions. In the case where the intramolecular interaction is antiferromagnetic (V′V′ and Ni′Ni′), weak intermolecular interactions, whatever their nature, do not influence the magnetic susceptibility data. On the other hand, in the case of Co′Co′, intermolecular interactions may contribute to the low-temperature susceptibility data together with the zero-field splitting within the triplet ground state. Finally, we emphasize that the susceptibility versus temperature and magnetization versus field data can be fitted with essentially the same sets of parameters, considering a pair model. This allows us to rule out the very unlikely hypothesis of significant intermolecular interactions.[33]

Discussion

Distribution of the Spin Density. As mentioned in the Introduction, the decamethylbimetallocenes M′M′ are model compounds for paramagnetic polymetallocenes. More precisely, the (η^5-C_5Me_5) ligands of M′M′ should indicate whether these

(32) See for example: (a) Bergerat, P.; Kahn, O.; Guillot, M. *Inorg. Chem.* **1991**, *30*, 1965−1966. (b) Caneschi, A.; Gatteschi, D.; Sessoli, R. *J. Am. Chem. Soc.* **1991**, *113*, 5873−5874. (c) Ménage, S.; Vitols, S. E.; Bergerat, P.; Kahn, O.; Girerd, J. J.; Xolans, X.; Calvet, T. *Inorg. Chem.* **1991**, *30*, 2666−2671.

(33) Bergerat, P.; Kahn, O.; Legoll, P.; Drillon, M.; Guillot, M. *Inorg. Chem.* **1994**, *33*, 2049−2051.

compounds deviate from the conventional metallocenes while allowing to analyze new features that are introduced by the fulvalene ligand.

Inspection of Table 2 and previous results of substituted metallocenes[8b,28b] show that in the case of V′V′ and Co′Co′ the ^{1}H and ^{13}C NMR signals of (η^5-C_5Me_5) appear in ranges which are characteristic of mononuclear vanadocenes and cobaltocenes. This is in perfect agreement with the temperature behavior of the reduced signal shifts (Figure 5) and with the magnetic results discussed below. By contrast, the (η^5-C_5Me_5) signals of Ni′Ni′ are found approximately halfway between those of mononuclear nickelocenes[8b,28] and 0 ppm owing to antiferromagnetic interaction (see below).

As for the bridging fulvalene ligand, the averaged NMR signal shifts of C1−5 and H2−5 resemble those of (η^5-C_5Me_5) except for C1−5 of V′V′ which experience a mean shift of more than 500 ppm to high frequency. More strikingly, the signal splitting for C1−5 and H2−5 of Ni′Ni′ and that for C1−5 of V′V′ is much larger than found previously for vanadocenes and nickelocenes having one substituent per Cp.

A qualitative understanding of the signal splitting has been shown to be related to the ligand π orbitals and their squared C2p_z coefficients.[8,28b,29b] From calculations carried out for the decamethylbimetallocenes (see below) it is clear that the MOs following the HOMO of Fe′Fe′ at increasing energies contain the fulvalene-type orbitals b_u, b_g/a_u, and a_g (Figures 11 and 12). These MOs should be concerned when the two and four additional electrons of Co′Co′ and Ni′Ni′, respectively, are arranged in various ways. The ^{13}C and ^{1}H NMR signal patterns which are expected for spin in a given orbital is visualized in Figure 9, traces a−l. The patterns were obtained by calculating the hyperfine coupling constants A(^{13}C)[32a] and A(^{1}H)[34b] from the Hückel coefficients of the fulvalene ligand in Ni′Ni′. To compare the *A* values with the NMR results both were scaled: the largest of all *A*(^{13}C) and *A*(^{1}H) values respectively, and the largest δ(^{13}C) and δ(^{1}H) values of each NMR spectrum were set equal to 1. This procedure eliminated the problem that the calculation of A assumes one unpaired electron per orbital, while in the compounds M′M′ the overall spin density on the fulvalene ligand is smaller and depends on M. MO calculations on the other molecules M′M′ showed that the respective NMR signal patterns are rather similar to those of Ni′Ni′ in Figure 9, traces a−l. Note that the resulting patterns (Figure 9, traces a−c and d−f) are inverted when the sign of the spin magnetic moment is inverted arbitrarily (traces g−i and j−l). As for the comparison with the experimental results (traces m−r), it is obvious that the 2/2/1 pattern of ^{13}C is more decisive than the 1/1 pattern of ^{1}H.

Obviously, the ^{13}C NMR results of Ni′Ni′ and Co′Co′ (traces m and n) cannot be reproduced by positive[8b,29b,35] spin located in only one of the orbitals a_g, b_g/a_u, and b_u, respectively (traces a−c). Note that spin in the similar MOs b_g and a_u (Figure 12) yields very similar patterns and that mean patterns are given in Figure 9 (traces b, e, h, and k). When we allow spin in two orbitals (from two or more unpaired electrons and/or thermally populated states), it turns out that only the combination of a_g and b_g/a_u leads to exclusively positive signal shifts and a 2/2/1 pattern as found for Ni′Ni′ and Co′Co′. Thus, for Ni′Ni′, the

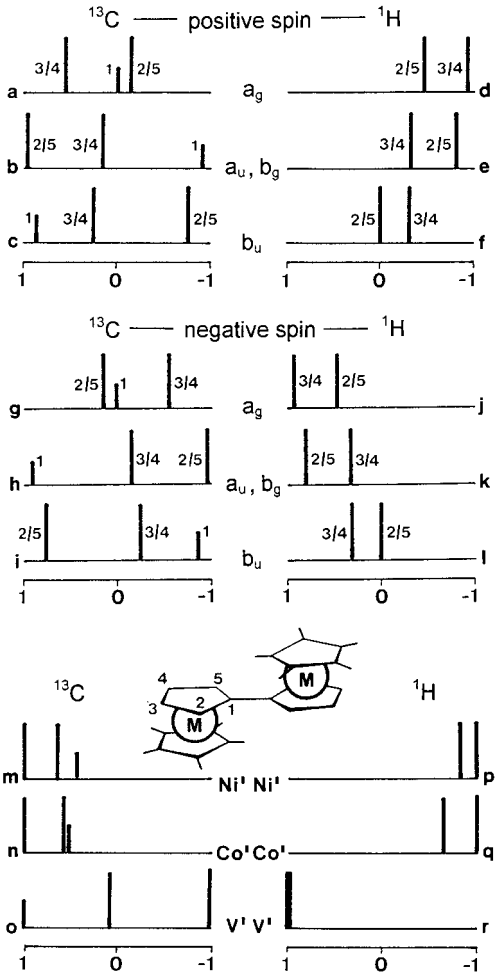

Figure 9. NMR signal patterns calculated[34] for unpaired electron spin in the a_g, a_u, b_g, and b_u orbitals (see also Figures 11 and 12) of Ni′Ni′. Other M′M′ give similar patterns. (a−c) ^{13}C NMR patterns, (d−f) ^{1}H NMR patterns, both series for positive spin in the MOs. (g−i and j−l) As previous traces, but for negative spin in the MOs. For comparison the experimental patterns for M′M′ are given in (m−r). All patterns are normalized to the largest signal shifts.

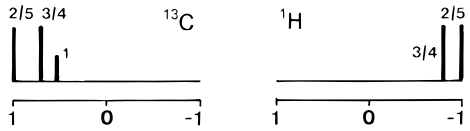

Figure 10. NMR signal patterns calculated for positive unpaired electron spin in the MOs b_g, a_u, and b_u of Ni′Ni′ (see text).

admixture of 47% of b_g/a_u and 53% of b_u yields the patterns shown in Figure 10 which agree well with traces m and p in Figure 9. On this basis the NMR signals of H2/5 and H3/4 as well as those of C2/5 and C3/4 were distinguished for Ni′Ni′ and Co′Co′. Although the calculated ^{13}C pattern of Figure 9 is very sensitive to the mixture of orbitals, the reasoning given here is meant to serve as a qualitative guide; a small contribution of spin in the a_g ligand orbital cannot be excluded.

As for V′V′ we know that the spin on the ligand is negative. Then, the experimental ^{13}C NMR spectrum (Figure 9, trace o) is best reproduced by trace h of Figure 9, which also establishes the signal assignment. We conclude that spin is induced in (lower-lying bonding) MOs which have fulvalene contents similar to those of the a_u and b_g orbitals shown in Figure 12. When the ^{1}H NMR result (Figure 9, trace r) is compared accordingly with trace k, it becomes evident that there are

(34) (a) Yonezawa, T.; Kawamura, T.; Kato H. *J. Chem. Phys.* **1969**, *50*, 3482−3492. (b) Drago R. S. *Physical Methods in Chemistry*; Saunders: Philadelphia, 1977; Chapter 9. (c) Ouishi, S.; Nitta, I. *J. Chem. Phys.* **1963**, *39*, 2848−2849.

(35) (a) Kollmar, C.; Kahn, O. *J. Chem. Phys.* **1992**, *96*, 2988−2997. (b) Blümel, J.; Hebendanz, N.; Hudeczek, P.; Köhler, F. H.; Strauss, W. *J. Am. Chem. Soc.* **1992**, *114*, 4223−4230 and references therein.

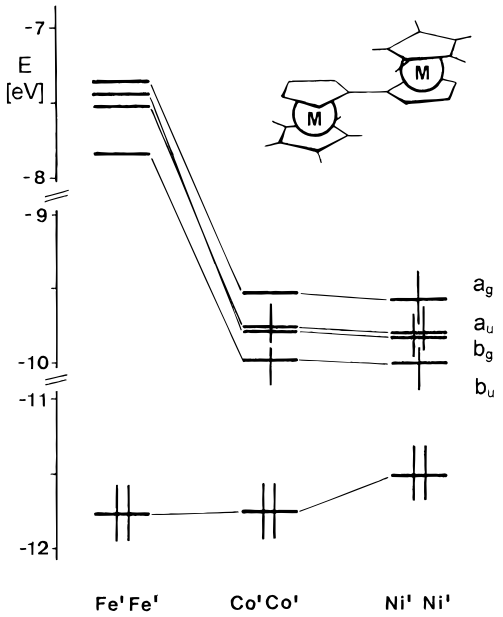

Figure 11. MO diagram of M′M′ showing the HOMO and the four next-highest (partly occupied) MOs for M = Fe, Co, and Ni.

additional contributions to the signal shifts, e.g., spin in σ orbitals.[36]

Magnetic Interaction. We were unable to grow crystals suitable for X-ray structure determination, but we can safely assume that the two Cp halves of the fulvalene bridge of all molecules M′M′ are coplanar and that the metals are trans with respect to the bridge as has been found for Fe′Fe′.[21a] In *trans*-M′M′ the metals are more than 5.2 Å apart, and therefore direct metal−metal interaction should not contribute significantly to the magnetic interaction. Rather, the interaction is expected to be ligand promoted.

To check this, extended Hückel MO calculations were carried out. At first, Fe′Fe′ was calculated as a reference compound. As expected, the results were similar to those obtained previously for the nonmethylated biferrocene which has been studied with respect to the photoelectron spectra and the structure.[37] When proceeding to Co′Co′ and Ni′Ni′ considerable changes were found which are illustrated in Figure 11. The four lowest empty MOs (b_u, b_g, a_u, and b_g) become less antibonding, and their splitting decreases when passing to Co′Co′ and Ni′Ni so that they may be regarded as quasi-degenerate. In particular, the relative ordering of the b_g and a_u orbitals is not reliable, because it depends on subtle changes of the interaction between the AOs at C1 and C2/5 described in more detail below. A naive arrangement of electrons would yield $S = 1$ for Co′Co′ and $S = 2$ for Ni′Ni′. Experimentally it turns out that the orbital splitting of Ni′Ni′ is big enough to manifest itself as antiferromagnetic interaction, whereas an accidental degeneracy of orbitals must be assumed for the ferromagnetically coupled Co′Co′.

In Figure 12 the shapes of the MOs are reproduced which are relevant for the magnetic interaction. We can confine the discussion to the fulvalene bridge as being composed of two reduced-spin Cp radicals (cf. Introduction). Accordingly and for clarity, in Figure 12 all other atomic orbital contributions

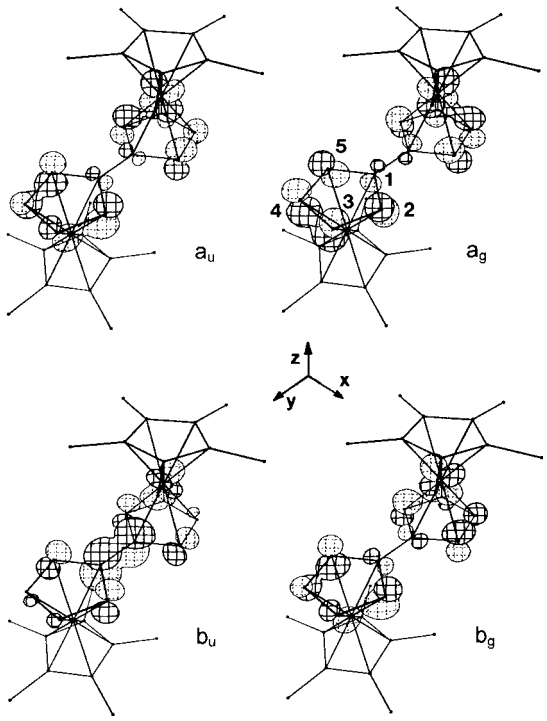

Figure 12. MOs of M′M′ relevant for magnetic interaction and the NMR patterns of Figure 9. Only selected AO contributions are given (see text).

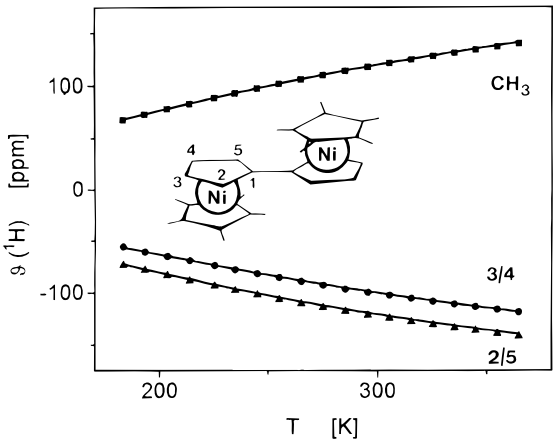

Figure 13. Temperature dependence of the reduced paramagnetic ^{1}H NMR signal shifts of Ni′Ni′. The curves are obtained by fitting the experimental data to eq 2.

were omitted except for one metal orbital just to show the relative metal content of the MOs and that they are metal−ligand antibonding. The a_g orbital is expected to favor ferromagnetic interaction because it is composed of two Cp-type orbitals which are orthogonal. However, it will be hardly populated even in Ni′Ni′. As for the a_u and b_g orbitals, the relative importance of two orbital interactions between the coupled metallocenes is crucial: the $2p_x$ orbitals at the direct link C1/C1′ and the $2p_z$ orbitals of the pairs C2/C2′ and C5/C5′. The first are orthogonal in b_g while the others are orthogonal in a_u. When these AOs prevail, ferromagnetic interaction will again be favored. Otherwise the small overlap between the $2p_x$ AOs in the a_u orbital and the $2p_z$ AOs in the b_g orbital will lead to small antiferromagnetic interaction. Finally, in the b_u orbital there is a good overlap between the $2p_z$ AOs at C1 and C1′, and strong antiferromagnetic interaction is expected. Note that it is the delicate interplay of these orbitals which strongly affects the relative energy ordering of the b_g and a_u

(36) (a) Hebendanz, N.; Köhler, F. H.; Müller, G.; Riede, J. *J. Am. Chem. Soc.* **1986**, *108*, 3281−3289. (b) Köhler, F. H.; Schlesinger, B. *Inorg. Chem.* **1992**, *31*, 2853−2859.

(37) (a) Böhm, M. C.; Gleiter, R.; Delgado-Pena, F.; Cowan, D. O. *J. Chem. Phys.* **1983**, *79*, 1154−1165. (b) Kirchner, R. F.; Loew, G. H.; Mueller-Westerhoff, U. T. *Inorg. Chem.* **1976**, *11*, 1665−2670.

orbitals (Figure 11) depending on the calculation method. As for V′V′ it was concluded that the spin resides in MOs which resemble the a_u and b_g orbitals. Therefore, the magnetic interaction should be weak, which was actually found.

In the previous section the spin density distribution was derived from NMR data. A limitation of the method is that it integrates over all MOs which contain unpaired electrons. In particular, it cannot be distinguished by the sequence of the ^{13}C NMR signals whether the b_g or the a_u orbital (or both) is engaged. Also, at the present time, the correlation between the NMR data and the spin densities is not precise enough as to determine the above-mentioned interactions between C1/C1′, C2/C2′, and C5/C5′.

Comparison of the NMR and the Magnetic Data. It is well-known that the contact shift δ^{con} is proportional to the magnetic susceptibility χ[38] and that this relation is also valid for exchange-coupled systems.[39] Here we apply it to Ni′Ni′, where two nickelocenes are coupled which each have $S = 1$. The reduced contact shift of a proton signal at a given temperature T takes the form[39]

$$\vartheta(^1H) = \delta^{con}{}_T(^1H)T = A(^1H)\frac{g_e{}^2\beta_e{}^2}{\gamma_H hk}\frac{3\exp(J/kT) + 5\exp(3J/kT)}{1 + 3\exp(J/kT) + 5\exp(3J/kT)} \quad (2)$$

where $A(^1H)$ (in tesla) is the sum of the hyperfine coupling constants of the observed proton with its neighboring and its own nickelocene fragment, g_e is the mean electron Zeeman factor, γ_H is the proton gyromagnetic ratio, J is the magnetic interaction parameter, and the other symbols have their usual meanings. Fitting of the temperature-dependent NMR signal shifts to eq 2 gives J and $A(^1H)$. This corresponds to obtaining J from a fit of solid-state magnetic data as can be seen from eq 3:

$$\delta^{con} = \frac{A}{2\gamma hN}\chi_m = \frac{A}{2g_n\beta_n N}\chi_m \quad (3)$$

where N, g_n, and β_n are Avogadro's number, the nuclear g factor, and the nuclear magneton, respectively. In the most common case of ^1H NMR the reduced proton signal shift is $\vartheta(^1H) = 0.988\ A(^1H)\chi_m T$.

Fitting of the experimental ^1H NMR data of Ni′Ni′ to eq 2 gave the $\vartheta(^1H)$ vs T curves in Figure 11 and the data in Table 3. The J values deviate up to 15 cm^{-1} from that obtained by the magnetic measurements. This is partly due to the temperature range which is much smaller for NMR work in solution than for solid-state magnetic measurements. Actually, when the $\chi_m T$ data are limited to $182 < T < 290$ K, i.e., a temperature range similar to that of the NMR measurements, J changes from -180 cm^{-1} (full temperature range) to -175 cm^{-1}.

The plausibility of the NMR results can be further checked by looking at the fit parameter A. As can be seen from eq 2, A corresponds to the reduced NMR signal shift that would result if the spins on the linked nickelocenes in Ni′Ni′ were independent. Hence these shifts are obtained as limiting signal shifts ($\vartheta(^1H)_\infty$) at infinite temperature; they are also listed in Table 3. It is gratifying that the $\vartheta(^1H)_\infty$ values are not far from the signal shifts of simple nickelocenes, e.g. $\vartheta(^1H) = 240$ for decamethylnickelocene.

Table 3. Magnetic Interaction Parameter (J), Hyperfine Interaction (A), and Limiting Signal Shift (ϑ_∞) Data for Ni′Ni′ Obtained by ^1H NMR Spectroscopy

	H2/5	H3/4	C*CH*$_3$
J [cm^{-1}]	−192	−165	−187
$A(^1H)$ [mT]	−0.121	−0.129	0.139
$\vartheta(^1H)_\infty$ [ppm]	−237	−252	272
J [cm^{-1}][a]	−180	−180	−180
$A(^1H)$ [mT]	−0.114	−0.140	0.134
$\vartheta(^1H)_\infty$ [ppm]	−223	−274	262

[a] Fixed value obtained from magnetic measurements.

Alternatively, the experimental data was fitted to eq 2 after setting $J = -180$ cm^{-1}, which was obtained from the magnetic measurements. The corresponding $A(^1H)$ and $\vartheta(^1H)_\infty$ values are given in the lower part of Table 3. Again they lie in the expected signal shift range.

When J is determined by NMR measurements its precision and scatter are influenced by all phenomena that render the hyperfine coupling and J itself temperature dependent. An example is inter- and intramolecular dynamic behavior. In the present case the two nickelocene fragments of Ni′Ni′ are expected to undergo a torsional vibration relative to each other.

We have extended the MO calculations described in the previous section to decamethylbimetallocenes in which the angle between the two metallocenes is changed by torsion about the central bond C1−C1′. A rather soft increase in energy was found when M′M′ departs from the trans arrangement. This is similar to the parent molecule fulvalene[40] but different from biphenyl.[41] Increasing temperature would thus populate twisted structures and modulate the interaction between the metallocene fragments.

Conclusions

The fulvalene dianion is an appropriate starting compound for the synthesis of reactive open-shell bimetallocenes having different metals. Ligand exchange may render these molecules unstable, a problem that can be circumvented for nickel by methylation. Hence the decamethylbimetallocenes M′M′ are best suited to study interactions between two directly linked metallocenes.

Upon coupling two metallocenes remarkable color changes may occur (Ni′Ni′), and the magnetic behavior changes as well. The magnetism is reflected in temperature-dependent NMR and susceptibility studies. The latter are more precise and more generally applicable. NMR studies have their merits when the purity of the compounds is checked, when their structures are confirmed, and when the spin-carrying orbitals are of interest.

The magnetism of M′M′ varies considerably. While V′V′ and Ni′Ni′ are weakly and strongly antiferromagnetically coupled, respectively, Co′Co′ is exceptional in featuring ferromagnetic interaction between two purely organometallic fragments. The magnetic interaction may be understood after identifying the MOs which contain the unpaired electrons and by analyzing the bridging ligand content in these MOs. This is a new example for treating paramagnetic organometallic compounds as reduced-spin organic radicals.

(38) La Mar, G. N.; Horrocks, W. DeW., Jr.; Holm, R. H., Eds. *NMR of Paramagnetic Molecules*; Academic Press: New York, 1973; Chapter 1. The sign convention has changed since.

(39) (a) Dunham, W. R.; Palmer, G.; Sands, R. H.; Bearden, A. J. *Biochim. Biophys. Acta* **1971**, *253*, 373−384. (b) La Mar, G. N.; Horrocks, W. DeW., Jr.; Holm, R. H., Eds. *NMR of Paramagnetic Molecules*; Academic Press: New York, 1973; Chapter 7. (c) Banci, L.; Bertini, I.; Luchinat, C. *Struct. Bonding* **1990**, *72*, 113−136. The sign convention has changed since.

(40) Streets, D. G.; Berkowitz, J. *Chem. Phys.* **1977**, *23*, 79−85.

(41) Rubio, M.; Merchán, M.; Orté, E. *Theor. Chim. Acta* **1995**, *91*, 17−29 and literature cited therein.

Experimental Section

All compounds were synthesized and investigated under purified dinitrogen by applying combined cannula/Schlenk techniques. The glassware was flame-dried in vacuo, and oxygen-free and dry solvents were used. The melting points were determined in sealed capillaries, and the elemental analyses were carried out by the Inorganic Microanalytical Laboratory at Garching. Published procedures were followed for the synthesis of the dilithium[9] and the dithallium[10] salts of the fulvalene dianion (**2** and **3**, respectively), $CpNiCl[P(OCH_3)_3]$,[15] (η^5-C_5Me_5)Co(acac),[18] (η^5-C_5Me_5)Ni(acac),[18] and [(η^5-C_5Me_5)-CoCl]$_2$.[19]

Reaction of $CpNiCl[P(OCH_3)_3]$ with Dithallium Bicyclopentadienyldiide. To a stirred solution of $CpNiCl[P(OCH_3)_3]$ (2.0 g, 7.1 mmol) in 100 mL of THF was added **3** (1.9 g, 3.6 mmol) at 25 °C. After a few minutes the solution turned deep red-violet and a white precipitate (TlCl) formed. After the solution was stirred for 2 h and passed through a frit, THF was removed in vacuo, and the residue was extracted with hexane. Stripping the solvent gave a red-brown solid which was a mixture of binickelocene (NiNi) (80%), ternickelocene (6%), bisfulvalenedinickel (3%), and nickelocene (11%) according to the ^{1}H NMR spectrum (Figure 1a) taken immediately after dissolution in C_6D_6. MS (*m*/*z* (%)): 374 (100) $[NiNi]^{2+}$.

Decamethylbiferrocene (Fe′Fe′). Solid $Fe_2Cl_4(THF)_3$ (8.56 g, 18.2 mmol) was added to a suspension of **2** (880 mg, 6.2 mmol) and (C_5Me_5)Na (9.36 g, 60.9 mmol) at 25 °C. The mixture, which turned orange after a few minutes, was stirred for 18 h. For workup the THF was stripped, the residue was extracted with 300-mL portions of hexane until the solution was colorless, and the combined extracts were freed from the solvent. Sublimation at 2 μbar and 80 °C bath temperature gave 7.5 g of (η^5-C_5Me_5)$_2$Fe, leaving behind 790 mg of an orange powder. A 400 mg amount of this material was dissolved in hexane and subjected to medium-pressure liquid chromatography using equipment described earlier[13b] (column length/diameter 15/3 cm, silica gel 0.063−0.02 μm). The first of three phases contained 10 mg of (η^5-C_5Me_5)$_2$Fe, the second one contained 220 mg of Fe′Fe′ (yield 14%, relative to **2** and scaled to the chromatographed sample), and the third one contained 180 mg of decamethylterferrocene Fe′FeFe′ together with a small amount of higher-nuclear species. Data for Fe′Fe′: Mp 310−312 °C. MS(CI) (*m*/*z* (%)): 510 (100), M^+; 347(3), $M^+ - C_5HMe_5$. ^{1}H NMR (C_6H_6) δ: 1.72 (s, 30H) CH_3; 3.66 (vt, ^{3+4}J(HH) = 3.4 Hz, 4H) H3/4; 3.73 (vt, ^{3+4}J(HH) = 3.4 Hz, 4H) H2/5. ^{13}C NMR (C_6D_6) δ: 11.0, CH_3; 68.4, C3/4; 71.7, H2/5; 80.2, C_5Me_5; 83.2, C1. The assignment of H2−5 follows that of biferrocene,[26] and a COSY experiment established the assignment of C2−5.

Anal. Calcd for $C_{30}H_{38}Fe_2$: C, 70.61; H, 7.51; Fe, 21.89. Found: C, 70.55; H, 7.48; Fe, 21.55. Data for Fe′FeFe′, ^{1}H NMR (C_6D_6) δ: 1.66 (s, 30H) CH_3; 3.67, 3.73, 4.02, 4.08 (each vt, ^{3+4}J(HH) = 3.4 Hz, 4H) H3/4, H2/5, H8/9, H7/10, respectively. The assignment of H3−10 is analogous to that of Fe′Fe′ and of biferrocene.[26]

Decamethylbicobaltocenium Bis(hexafluorophosphate) ($[Co′Co′]^{2+}$-$[PF_6]^-_2$). A solution of [(η^5-C_5Me_5)CoCl]$_2$ (2.18 g, 4.8 mmol) in 100 mL of THF and a suspension of **3** (2.46 g, 4.6 mmol) in 100 mL of THF were cooled to −35 °C. The solution was added to the suspension via cannula, then the mixture was stirred for 1 h and allowed to warm to room temperature after removing the cooling bath. Subsequently the solvent was removed in vacuo, 150 mL of water was added to the olive-green solid, and the mixture was passed through a frit in order to separate thallium. When an excess of NH_4PF_6 (1.8 g, 11 mmol) was added to the solution a precipitate formed. Recrystallization from hot acetonitrile gave 3.50 g (95% yield) of yellow crystals of $[Co′Co′]^{2+}$-$[PF_6]^-_2$. MS (FD, acetone) (*m*/*z* (%)): 661 (67) $[(C_5Me_5)_2Co_2(Co_{10}H_8)PF_6]^+$; 516 (100) $[(C_5Me_5)_2Co_2(C_{10}H_8)]^+$. ^{1}H NMR (acetone-$d_6$) δ: 1.91 (s, 30H) CH_3; 5.80 (vt, ^{3+4}J(HH) = 4.2 Hz) H3/4; 5.99 (vt, ^{3+4}J(HH) = 4.2 Hz) H2/5. Anal. Calcd for $C_{30}H_{38}Co_2F_{12}P_2$: C, 44.68; H, 4.75; Co, 14.62; F, 28.27; P, 7.68. Found: C, 44.56; H, 4.79; Co, 14.00; F, 25.94; P, 6.88.

Decamethylbicobaltocene (Co′Co′). Method I. Solid (η^5-C_5Me_5)-Co(acac) (1.93 g, 6.6 mmol) was added to a stirred solution of **2** (480 mg, 3.3 mmol) in 150 mL of THF which was cooled to −78 °C. When the mixture was allowed to warm to room temperature during 15 h the color changed from yellow-brown to dark brown. Stripping of THF gave a solid which was extracted with 150 mL of hexane. Upon concentration and cooling a powder formed which was recrystallized several times to give dark brown microcrystals of Co′Co′ (320 mg, 19%).

Method II. Sodium amalgam (1.94 wt % Na) (3.16 g, 2.68 mmol Na) was added to a yellow suspension of $[Co′\ Co′]^{2+}[PF_6]^-_2$ (1.07 g, 1.3 mmol) in 70 mL of THF. In the course of 3 days the color changed to green and then to dark brown. The solid which was obtained after stripping THF was extracted with hexane until the fraction was colorless, and the solvent was removed from the combined extracts under reduced pressure to give dark brown microcrystals of Co′Co′. The yield after recrystallization was 600 mg (88%), mp 285 °C; Co′Co′ decomposed partly above 255 °C upon slow heating. MS (*m*/*z* (%)): 516 (100), M^+; 380 (18), $M^+ - (C_5Me_5) - H$; 258 (33), M^{2+}; 187 (2), $[Co(C_{10}H_8)]^+$. Anal. Calcd for $C_{30}H_{38}Co_2$: C, 69.76; H, 7.42; Co, 22.82. Found: C, 69.42; H, 7.60; Co, 21.2.

Decamethylbinickelocene (Ni′Ni′). The procedure was analogous to method I described for Co′Co′. Thus 660 mg (4.7 mmol) of **2** and 2.73 g (9.3 mmol) of (η^5-C_5Me_5)Ni(acac) gave 360 mg (15% yield) of Ni′Ni′ as dark violet powder which melted at 260 °C and slowly decomposed above 230 °C. MS (*m*/*z*(%)): 515 (100), MH^+; 379 (44), $M^+ - (C_5Me_5)$; 258 (17), MH_2^{2+}; 244 (5), $[Ni_2(C_{10}H_8)]^+$; 186 (7), $[Ni(C_{10}H_8)]^+$; 58 (4), Ni. Anal. Calcd for $C_{30}H_{38}Ni_2$: C, 69.82; H, 7.42; Ni, 22.75. Found: C, 69.35; H, 7.45; Ni, 22.62.

Decamethylbivanadocene (V′V′) and Octadeuteriodecamethylbivanadocene (V′V′-d_8). $VCl_3(THF)_3$ (7.08 g, 18.9 mmol) and zinc dust (3.10 g, 47.4 mmol) were suspended in 150 mL of THF and stirred at 25 °C for 48 h. The brown solution was removed from the resulting mixture via cannula, and the light green solid was washed twice with 150 mL of THF, suspended in 200 mL of THF, and reacted with a THF solution of **2** (660 mg, 4.7 mmol) and (C_5Me_5)Li (4.00 g, 28.1 mmol). The mixture, which turned red-brown, was stirred for 48 h, THF was removed under reduced pressure, and the remaining solid was extracted with 250 mL of hexane. After the hexane was stripped from the solution, 1.25 g of (η^5-C_5Me_5)$_2$V was removed from the solid by sublimation (1 μbar, 80 °C bath temperature). Renewed extraction of the remainder with hot hexane and stripping the solvent gave brown microcrystals of V′V′ (580 mg, 25% yield), which melted at 263 °C and slowly decomposed above 235 °C. MS (*m*/*z* (%)): 500 (100), M^+; 362 (40), $C_{20}H_{23}V_2^+$; 250 (12), M^{2+}; 179 (1), $[V(C_{10}H_8)]^+$. Anal. Calcd for $C_{30}H_{38}V_2$: C, 71.22; H, 7.65. Found: C, 71.39; H, 7.67.

The synthesis of the deuterated analogue started from cyclopentadiene-d_6[36b] which was converted to **2**-d_8 following literature procedures.[9] Further reaction as described for V′V′ using 14.4 g (38.5 mmol) of $VCl_3(THF)_3$, 4.65 g (71 mmol) of Zn, 9.68 g (68 mmol) of (C_5Me_5)Li, and 1.52 g (10.1 mmol) **2**-d_8 gave 1.19 g of V′V′-d_8 (yield 23%).

Physical Measurements and MO Calculations. The mass spectra were run with Finnigan MAT 90 and Varian MAT 311 A instruments employing the election impact mode (70 eV) unless stated otherwise. The reported ions were calculated using the rounded masses of the most abundant isotopes. The NMR spectra were recorded on a JEOL JNM GX 270, a Bruker CXP 200, and a Bruker MSL 300 spectrometer. The paramagnetic samples were measured in standard tubes equipped with ground glass and stoppers, except for the ^{13}C NMR spectra which were obtained with tubes described previously.[42] The temperature was calibrated by using Pt resistance thermometer devices (Lauda R 42 and Merz MN 100) with the probe being placed in an NMR tube which contained ethylene glycol. All signals were measured relative to solvent peaks and their paramagnetic shifts, δ^{para}, calculated relative to the signal shifts of the corresponding nuclei of Fe′Fe′ by using known solvent shifts.[43] The standard values $\delta^{para}{}_{298}$ were interpolated from temperature-dependent measurements. The UV/vis spectra were recorded on a Perkin-Elmer Lambda 2 spectrometer. The magnetic susceptibility and magnetization measurements were carried out with a SQUID magnetometer working in the 1.7−300 K temperature range and (0−80) × 10^3 Oe field range. The samples were sealed in quartz tubes under

(42) Köhler, F. H.; Metz, B.; Strauss, W. *Inorg. Chem.* **1995**, *34*, 4402−4413.

(43) Kalinowski, H.-O.; Berger, S.; Braun, S. *^{13}C NMR-Spektroskopie;* Georg Thieme Verlag: Stuttgart, 1989; p 74.

vacuum. The data were corrected for the magnetization of the sample holders and for the core diamagnetism. The MO calculations were carried out by using the program CACAO of C. Mealli and D. M. Prosperio,[44] Version 4.0, 1994. The molecular geometries were derived from the structure of Fe′Fe′ [21a] and the known metal−ligand distances of the other metallocenes.[45]

(44) Mealli, C.; Prosperio, D. M. *J. Chem. Educ.* **1990**, *67*, 399−402.
(45) Haaland, A. *Acc. Chem. Res.* **1979**, *12*, 415−422.

Acknowledgment. We thank Drs. J. Blümel, G. Raudaschl-Sieber, and A. Steck for measuring the CP MAS NMR, the UV/vis, and the NOE spectra, respectively. This work was supported by the Deutsche Forschungsgemeinschaft, the European Union (HCM Network, "Magnetic Molecular Materials"), and the Fonds der Chemischen Industrie.

IC980332T